TOPICAL REVIEW — 8th IUPAP International Conference on Biological Physics

Amyloid-β peptide aggregation and the influence of carbon nanoparticles*

Wen-Hui Xi(郗文辉) and Guang-Hong Wei(韦广红)†

Key Laboratory for Computational Physical Sciences (Ministry of Education), State Key Laboratory of Surface Physics, Department of Physics, Fudan University, Shanghai 200433, *China*

(Received 12 May 2015; revised manuscript received 16 August 2015; published online 30 November 2015)

Soluble peptides or proteins can self-aggregate into insoluble, ordered amyloid fibrils under appropriate conditions. These amyloid aggregates are the hallmarks of several human diseases ranging from neurodegenerative disorders to systemic amyloidoses. In this review, we first introduce the common structural features of amyloid fibrils and the amyloid fibrillation kinetics determined from experimental studies. Then, we discuss the structural models of Alzheimer's amyloid-β (Aβ) fibrils derived from solid-state nuclear magnetic resonance spectroscopy. On the computational side, molecular dynamics simulations can provide atomic details of structures and the underlying oligomerization mechanisms. We finally summarize recent progress in atomistic simulation studies on the oligomerization of Aβ (including full-length Aβ and its fragments) and the influence of carbon nanoparticles.

Keywords: Amyloid-β, oligomerization, carbon nanoparticles, molecular dynamics

PACS: 87.14.em, 87.15.nr, 87.15.bk, 87.15.ap **DOI:** 10.1088/1674-1056/25/1/018704

1. Introduction

Amyloid fibrillar aggregates, formed by the self-aggregation of peptides/proteins, not only have biological functions in certain organisms,[1] but also are one of the hallmarks of several human diseases ranging from neurodegenerative disorders to systemic amyloidoses.[2] More than 20 human diseases are associated with the pathological self-assembly of amyloid-forming peptides/proteins, such as Alzheimer's Disease (AD),[3] Parkinson's Disease (PD),[4] transmissible spongiform encephalopathy (TSE),[5] Huntington's Disease,[6] and type II diabetes (T2DM).[7] For each disease, a specific protein is involved in amyloid fibril formation. Some of the aggregation-prone peptides/proteins have a well-defined three-dimensional (3D) structure in solution, while some are intrinsically disordered peptides/proteins (IDPs),[8] which typically consist of multiple charged residues and a few hydrophobic residues. Intensively-studied amyloidogenic IDPs include the amyloid-β (Aβ) peptide (37–43 amino acids [aa],[9] associated with AD), tau protein (441 aa,[10] related to AD), the human islet amyloid polypeptide (37 aa,[11] associated with T2DB), and alpha-synuclein (140 aa, associated with PD).[12] Although the amyloidogenic proteins have different amino acid sequences and biophysical properties in solution, they all self-aggregate into thin and long amyloid fibrils, indicating their common structural feature[13] and aggregation mechanism. Although amyloid deposits are the hallmarks of many human diseases, a growing body of evidence suggests that the fibrillation process itself and the early formed small oligomers are also cytotoxic.[14,15] However, due to the transient nature of the oligomers, it is challenging to characterize their structures experimentally. As a complement to experimental methods, molecular dynamics (MD) simulations can provide atomic details of structures and the underlying oligomerization mechanism. In this review, we first introduce the common structural feature of amyloid fibrils and the amyloid fibrillation kinetics. We then discuss the structural models of Aβ fibrils derived from solid-state nuclear magnetic resonance (ss-NMR). Finally, we summarize recent progress in atomistic simulation studies on the oligomerization of Aβ (including full-length Aβ and its fragments) and the effects of carbon nanoparticles.

2. Experimental characterization of peptide aggregation

2.1. The cross-β structure of amyloid fibrils

Based on the results of x-ray diffraction experiments, amyloid fibrils are known to be characterized by a cross-β structure, with the β-strands perpendicular to and the inter-strand hydrogen bonds parallel to the fibril axis[16,17] (for more details about the cross-β structure, see Fig. 1 and its figure caption). However, due to the limited structural order of fibrils, it is difficult to determine the atomic details of the cross-β spine using x-ray crystallography, solution NMR, or electron microscopy (EM) methods. The architecture of the cross-β amyloid spines has been clarified by determining short segments of amyloidogenic proteins using microcrystals

*Project supported by the National Natural Science Foundation of China (Grant Nos. 11274075 and 91227102).

†Corresponding author. E-mail: ghwei@fudan.edu.cn

© 2016 Chinese Physical Society and IOP Publishing Ltd

of short peptides ($\leq$ 8 aa) by the Eisenberg group.[16,18] Fibril structural models of amyloidogenic proteins (including Aβ and human islet amyloid polypeptide [hIAPP]) have gradually emerged from studies using solid-state NMR.[19]

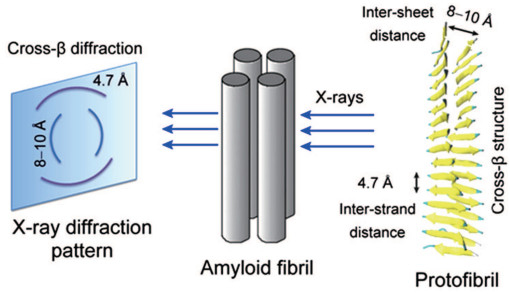


Fig. 1. A diagram showing the x-ray diffraction pattern and cross-β structure feature of fibrils. The characteristic cross-β diffraction pattern is generated when x-rays are directed on amyloid fibrils, which consist of multiple protofibrils. The diffuse reflection at 4.7 Å spacing along the meridian (vertical) shows extended protein chains running approximately perpendicular to the fibril axis and spaced 4.7 Å apart. The increasingly diffuse reflection at 8–10 Å spacing along the equator (horizontal) shows that the extended chains are organized into sheets spaced 8–10 Å apart. The cross-β structure can be seen from the cartoon representation of a protofibril.

2.2. The nucleation-dependent polymerization model of amyloid fibril formation

Understanding the self-aggregation process of amyloid peptides from soluble monomers/oligomers to insoluble amyloid fibrils is crucial for the investigation and treatment of amyloidosis. *In vitro* experimental studies of the kinetics of peptide aggregation have been carried out extensively.[20–22] The most well-accepted model is the nucleation-dependent polymerization model, where the fibrillation process produces a sigmoidal kinetic curve.[20,21] A schematic diagram of the fibrillation process is shown in Fig. 2. Amyloid fibrillation follows a two-step kinetics process (nucleation-elongation), which is characterized by a long lag phase associated with the formation of a nucleus and a rapid fibril elongation phase

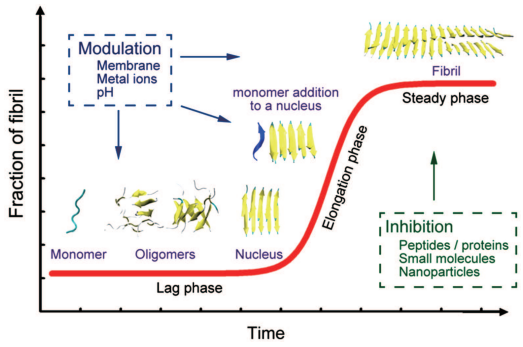


Fig. 2. A schematic diagram showing the nucleation-dependent polymerization model of amyloid fibril formation. During the lag phase (nucleation), monomeric forms of the amyloid-forming peptides self-aggregate into soluble oligomers (including disordered oligomers, β-barrels, and bilayer β-sheets) and nuclei. During the elongation phase, the nucleus is extended rapidly and grows into fibrils. Then, fibrillation reaches a stage called the steady phase. Aggregation processes produce a sigmoidal kinetic curve (red) that is depicted in the figure. Many factors can influence this fibrillation process.[26–28]

in which the nucleus rapidly grows into fibrils by the addition of monomers. After that, fibrillation reaches a stage called the steady phase, during which fibrils mature into amyloid deposits.[23,24] The lag phase during which nucleation occurs is the rate-limiting step and therefore controlling this step is important. Environmental conditions, such as membranes, metal ions, pH, and temperature, modulate the aggregation process.[25] Additionally, other factors, such as peptides/proteins, small molecules, and nanoparticles, can inhibit this process by disrupting intermolecular interactions.[26–28]

2.3. Structural models of Aβ fibrils derived from solid-state NMR

Alzheimer's amyloid plaques consist mostly of 40- and 42-aa(Aβ1–40 and Aβ1–42) peptides. Aβ1–42 is considered more toxic than Aβ1–40, although the latter is more abundant in neurons.[29] Since 2000, based on structural constraints from ss-NMR data, several structure models of Aβ fibrils have been proposed.

Based on ss-NMR data, Tycko group proposed the first structure model of the Aβ1–40 fibril in 2002.[30] Thereafter, structure models for Aβ1–42[31] and Aβ1–40[32] fibrils were reported by the Riek and Tycko groups, respectively. Since then, fibril structures of other amyloidogenic proteins or protein segments have been proposed, such as the structure models of hIAPP,[33] Tau proteins,[34] alpha-synuclein[35] fibrils. All of these fibrillar structures share a common cross-β structure feature in spite of their low sequence similarity. Aβ fibrils are mostly organized in parallel β-sheets, but antiparallel ones also exist.[36] Under different fibrillation conditions, Aβ1–40/1–42 monomers can assemble into polymorphic fibrils with different symmetries.[37]

Four extensively studied ss-NMR-derived Aβ fibrils are given in Fig. 3.[31,32,37,38] For clarity, figure 3 shows only the strands in the top layer of the fibril. These fibril structures all display a parallel β-strand-turn-β-strand (U-shaped) feature, although they have different symmetries, salt-bridge pairs, and side-chain packing patterns. The Aβ1–42 fibril model by the Riek group[31] (PDB id: 2BEG, Fig. 3(a)) is characterized by inter-molecular D23-K28 salt-bridges with an unstructured fragment from residues 1 to 16 (not shown). The N-terminal β1-strand (residues 18–26) and the C-terminal β2-strand (residues 31–42) are linked by a turn region spanning residues 27–30. The two Aβ1–40 fibril models by the Tycko group are unstructured for the first eight residues (not shown) and display two different symmetries: 2-fold[32] (PDB id: 2LMN, Fig. 3(b)) and 3-fold[37] (PDB id: 2LMP, Fig. 3(c)). The turn region linking the N-terminal (residues 9–24) and C-terminal (residues 30–40) β-strands spans residues 25–29. In the fibril structure with 3-fold symmetry, no salt-bridges exist between K28 and E22 or D23. Compared to these three

fibril models, the Aβ1–40 fibril structure from the brain tissue of AD patients[38] (PDB id: 2M4J, Fig. 3(d)) has less β-sheet content, with the N-/C-terminal β-strand region spanning residues 12–19/31–38. The different ss-NMR-derived structural models of Aβ fibrils reveal the polymorphism of Aβ fibrils.

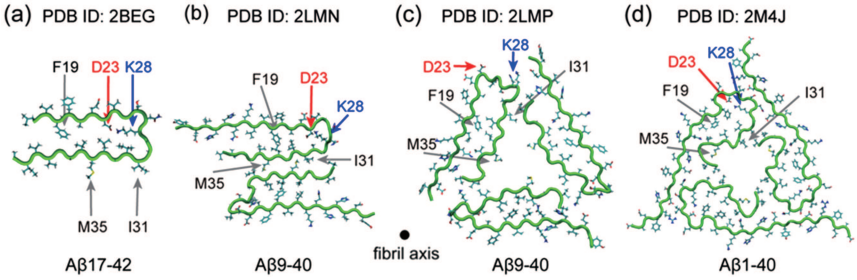


Fig. 3. Four Aβ fibril structural models derived from ss-NMR. (a) Aβ17–42 (PDB id: 2BEG),[31] (b) Aβ9–40 with 2-fold symmetry (PDB id: 2LMN),[32] (c) Aβ9–40 with 3-fold symmetry (PDB id: 2LMP),[37] (d) Aβ1–40 fibril from the brain of AD patients, with 3-fold symmetry (PDB id: 2M4J).[38]

3. Atomistic molecular dynamics studies of Aβ oligomerization

Molecular simulations on multi-level models are widely used in various fields, including physics, chemistry, and biology. The Noble Prize in Chemistry in 2013 was awarded to three scientists who developed multi-scale models for molecular simulations. For biomolecular systems, molecular simulations are powerful tools to study amyloidogenic peptide aggregation on different levels, ranging from the most precise quantum calculation to coarse-grained (CG) models. Computational studies of peptide aggregation on the atomistic level provide a balance between accuracy and computational cost and become prolific tools. In 2011, Shaw *et al.* performed a series of MD simulations on Anton with the AMBER ff99SB-ILDN force field and proved that the current force field performs well in general.[39]

Various computational techniques have been employed to study amyloidogenic peptide aggregation (reviewed in a recent paper[40]). The replica-exchange molecular dynamics (REMD) simulation method is particularly suited to sample the conformational space of short peptides The REMD method is an enhanced sampling protocol, in which several identical copies (replicas) of the system are simulated in parallel at different temperatures or at the same temperature but using different Hamiltonian and these replicas are periodically swapped with a probability given by the Metropolis criterion. This can avoid getting trapped in local-minimum free energy states.[41] The REMD method is useful for simulating complex problems such as protein folding and peptide aggregation. Since 2005, this method has been widely used in the study of amyloidogenic peptide aggregation.[42–44]

Due to its low computational cost, CG models have also been widely used in peptide aggregation, such as the OPEP[45] and PRIME models.[46] A detailed summary of the CG model used in peptide aggregation can be found in a recent review by Wu and Shea.[47] Here, we discuss recent progress of simulation studies using atom-level models by focusing on the oligomerization of Aβ peptides and its different fragments. Summaries of MD studies in this area in early years can be found in other reviews.[48,49]

3.1. Aggregation of amyloid-β peptide fragments

Certain fragments of amyloidogenic peptides have similar properties as their full-length counterpart and can aggregate into β-sheet-rich fibrils *in vivo* and retain their toxicity. These fragments are used widely as model systems to study peptide aggregation. Here, we briefly review MD studies on the monomeric and oligomeric forms of different Aβ fragments.

3.1.1. Structural stability of preformed fibrils

As early as 2002, Ma and Nussinov examined the structural stability of various constructed fibril models of different Aβ fragments (including Aβ16–22, Aβ16–35, and Aβ10–35) by MD simulations with the aim of characterizing the atomic structure of stable fibrils. Their MD simulations indicate that an antiparallel β-sheet orientation is the most stable for the Aβ16–22 peptide, consistent with a solid-state ss-NMR-based fibril model of the Aβ16–22 peptide.[50] Aβ16–22 is a peptide that contains the central hydrophobic core (CHC) motif (LVFFA) of full-length Aβ. For Aβ16–35 peptide, a bent double-layered hairpin-like parallel β-sheet structure was found to have higher structural stability. Residues D23 and K28 in the middle polar region of Aβ16–35 form an intra-chain salt-bridge and stabilize the double-strand conformation.[51] The effects of mutation on the fibril structural stability of Aβ fragments were also investigated. By building various parallel/antiparallel arrangements of β-sheet oligomers, Ma *et al.* compared the stability of the Aβ25–35 N27Q mutant with that of the wild type species[52] and found that a single mutation could reduce amyloid fibrillation propensity. MD simulations of the dissociation of Aβ16–22

monomers from preformed fibrils[53] were also reported.

3.1.2. Conformational distribution of the monomers of Aβ fragments

Numerous computational studies were initially focused on the conformational distribution of monomeric Aβ fragments. In 2006, Gnanakaran *et al*. explored the conformational space of the Aβ16–22 peptide by performing REMD simulations, and found that the predominant secondary structure is the PPII rather than the β-strand (PPII content $>$ 40%).[54] In the same year, using REMD simulations, Wei and Shea studied the free energy landscape of monomeric Aβ25–35 in both pure water and HFIP/water cosolvent. In water, the Aβ25–35 peptide mainly adopts collapsed coil conformations and to a lesser extent β-hairpins with a turn at G29–A30, while in the apolar organic HFIP solvent, this peptide preferentially populates a helical structure.[55]

The conformational distribution of various C-terminal fragments of Aβx–42 (x = 29–31, 39) were also studied by REMD simulations. These C-terminal Aβ fragments mostly adopt metastable β-hairpin conformations, except for Aβ39–42, which has an extended β-strand structure. Interestingly, when residues 40 and 41 are truncated from the Aβ30–42 fragment, the conformation shifts from β-hairpin to turn-coil state.[56] The folding energy landscape of the turn-region-containing peptide Aβ21–30 was studied by Baumketner *et al.* using REMD simulations.[42] Salt bridges were found to be formed between residues E22 and K28, instead of between D23 and K28. Using the same method, they also studied the influence of the E22/D23 mutation on the monomeric structures of Aβ21–30 and found that the E22 mutation does not alter the bend conformation while the D23 mutation converts the bend motif into a turn structure.[57] Similar results were also reported by Tarus *et al.*[58] Longer Aβ fragments, such as Aβ10–35,[59–61] Aβ12–28,[62] Aβ12–36,[63] and Aβ15–28,[64] have also been studied by MD simulations. Their relatively long aa sequences allow them to adopt multiple conformations, rather than having a single structure motif.[62,64,65]

3.1.3. Dimerization of Aβ fragments

A dimer is the smallest oligomer. Understanding the dimerization process of Aβ fragments provides structural insight into the early stage of amyloid fibrillation. In early years, due to the limitations of computational capability, dimeric systems became good model systems for understanding peptide aggregation. For example, in 2006, Gnanakaran *et al*. investigated the dimeric structures of Aβ16–22 by conducting atomistic REMD simulations. They found that Aβ16–22 dimers adopt various conformations, including parallel and antiparallel β-sheet structures.[54] The dimeric structures of Aβ25–35 were also studied with REMD simulations.[66,67] Various structures coexist in a balance of disordered compact states and extended fibril-like β-sheet conformations including parallel and antiparallel β-sheets, β-hairpins, and U-shaped β-sheets. Moreover, the stable parallel and antiparallel bilayer β-sheet protofibrils identified by MD simulations are consistent with experimental data from H/D exchange NMR and atomic force microscope spectroscopy.[67] Energetic analysis reveals that the formation of compact conformations is driven by entropy, while the fibril-like state is stabilized by inter-/intra-chain electrostatic interactions.[66] The dimerization of other Aβ fragments has also been studied by different simulation methods.[68,69]

3.1.4. Oligomeric structures of Aβ fragments

The increase of computational power in recent years allows researchers to investigate the conformational space of oligomers consisting of multiple peptide chains. For example, Li *et al.* explored the conformational distribution of Aβ16–22 octamers by performing explicit-solvent REMD simulations in a neutral-pH condition in 2011. They found that Aβ16–22 octamers adopt mostly disordered coil aggregates, and to a lesser extent, closed β-barrels and bilayer β-sheets.[70] Interestingly, one year later, the atomic view of cylindrical β-barrels formed by an 11-residue peptide was reported in an experimental study.[71] The octameric structures of Aβ16–22 in an acidic pH condition were studied by Xie *et al.* using explicit-solvent REMD simulations.[72] Similar to the octameric conformations at neutral pH,[70] disordered aggregates and ordered octamers (including closed β-barrels and bilayer β-sheets) were observed (see Fig. 4 for representative conformations).[72] The main stabilization forces for these ordered structures are hydrophobic and aromatic stacking interactions between F19–F19 and L17–F19 residues.[72] The structures of the longer Aβ fragment, Aβ25–35 oligomers, which range from monomer to tetramer, were also studied using REMD simulations by Larini *et al.*[73] Aβ25–35 preferentially forms β-hairpin conformations in its monomeric state and extended β-strand conformations in oligomeric states.[73]

The influence of force fields on the structures of Aβ fragments has been investigated by several groups. For example, Wang *et al*. studied the conformations of monomeric Aβ12–28 using two different models—OPLS–AA/TIP4P and GROMOS 43A1/SPC).[74] Structural analyses reveal that both models generate mostly random coil conformations with differences in the turn region of the β-hairpin (GROMOS 43A1: F19–E22; OPLS–AA: L17–F20). Thereafter, Nguyen *et al*. examined the structures of monomers, dimers, and trimers of Aβ16–22 with AMBER99, GROMOS96, and OPLS force fields.[75] Their REMD simulation results show that AMBER99 favors a helical structure, GROMOS96 has a bias to antiparallel β-sheet conformations, and OPLS reveals diverse structures. The different conformational bias of these force fields reminds us to be cautious when choosing a force field.

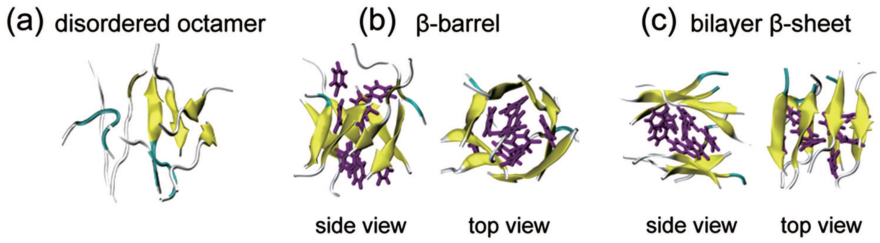


Fig. 4. Representative structures of Aβ16–22 octamers. (a) a disordered state, (b) a closed β-barrel structure in two different views, and (c) a bilayer β-sheet in two different views. The side chains of residues F19 and F20 are in purple stick representation. This figure is adapted from Ref. [72].

3.2. Conformational landscape of full-length Aβ peptide

Much effort has also been devoted to exploring the free energy landscape of the full-length Aβ peptide. For example, by performing implicit-solvent REMD simulations, Baumketner *et al*. found that Aβ42 monomer adopts extended structures consisting mainly of loops and turns and to a lesser extent helices in the C-terminal region.[76] This work demonstrates the feasibility of the REMD method in sampling the conformational space of the monomeric state of a full-length Aβ peptide. Soon after, many researchers focused on the study of conformational and thermodynamic properties of monomeric Aβ using REMD simulations.[77–83] Besides Aβ1–40/Aβ1–42 peptides,[77,79,81,82] Aβ peptides containing 39[78] and 43[83] residues were also analyzed. Comparing the conformational ensembles and free energy landscapes of the Aβ monomer, the differences between these four sequences are summarized as follows.

(i) All four sequences do not have unique folded structures but have a large conformational ensemble.

(ii) Aβ1–42 has a more structured C-terminal region than Aβ1–40. The C-terminal region spanning residues 31–42 preferentially adopts β-hairpin conformations.[77] Residues I41 and A42 have a propensity to interact with the central hydrophobic core (CHC) region.[79]

(iii) The D23–K28 salt-bridge is observed in Aβ1–40 but not in Aβ1–42.[84]

(iv) A turn region in segment 21–27 is found in Aβ11–39.[78]

(v) Residue T43 in Aβ1–43 can form a hydrogen bond with residue R5.[83]

MD and REMD simulations were also applied to compare various mutants (E22Q,[85] D23N,[86] D7H,[87] A2T/A2V[88]) with wild type Aβ. Simulation results show that these mutations significantly alter the conformational landscape of the Aβ monomer.[85]

The REMD method was also used to study full-length Aβ oligomers. In 2010, Kim *et al*. simulated Aβ1–40 monomers, dimers, and tetramers using implicit-solvent REMD simulations. Conformational analyses reveal sharp structural difference between monomers and oligomers.[89] Recently, the dimeric structures of full-length Aβ1–40/Aβ1–42 have been investigated using extensive explicit-solvent REMD simulations.[90–92] These studies report that the full-length Aβ dimer adopts various conformations with low α-helix and β-sheet content.

Knowing whether an Aβ fragment in its isolated form and this fragment within the full-length Aβ adopts similar conformations is important for understanding the role of the smaller fragment on the structure of full-length Aβ. A combined REMD and NMR study on Aβ1–42 and Aβ21–30 shows that Aβ1–42 adopts various conformations spanning from collapsed structured states to highly extended conformations, while Aβ21–30 has a relatively homogeneous ensemble of extended structures. This result indicates that Aβ21–30 in isolation and the 21–30 region in full-length Aβ has different conformational space.[93]

4. Inhibitory effect of carbon nanoparticles on Aβ aggregation

During the aggregation process of Aβ peptides, when additional factors (such as nanoparticles, metal ions,[94] and membranes) are involved in this process, they can modulate Aβ fibrillation. The regulation of Aβ aggregation by metal ions and membranes has been discussed in a recent review.[95] Here, we discuss only the effect of carbon-based nanoparticles on Aβ aggregation.

Nanoparticles have been reported to be able to influence amyloid formation.[96,97] There are three different kinds of carbon nanoparticles: carbon nanotubes, fullerenes, and graphites. Kim *et al*. found that fullerenes could inhibit the aggregation of Aβ11–25 and Aβ1–40.[98] Modified fullerenes were also able to prevent the aggregation of Aβ25–35 peptide.[99,100] Linse *et al.* reported that carbon nanotubes could enhance the fibril formation of the globular protein β2-microglobulin.[27] Graphites were shown to promote the formation of Aβ fibrils.[101–103]

In spite of a series of experimental studies, the molecular mechanism of carbon-nanoparticle-modulated aggregation of Aβ peptides is unclear. Here, we review recent atomistic MD studies on this topic. The atomistic MD study by Fu *et al*. in 2009, showed that a single-walled carbon nanotube (CNT) could induce two preformed bilayer β-sheets with

mixed antiparallel–parallel strands to assemble into a closed β-barrel wrapping the CNT. By analyzing the Aβ16–22–CNT interactions, the authors suggested that the β-barrel formation on SWNT surface results from the interplay of dehydration, peptide–CNT, and peptide–peptide interactions.[104] Two years later, Li *et al*. studied the interaction of another Aβ fragment–Aβ16–22 with CNT by REMD simulations in explicit solvent.[70] Their simulations showed that CNTs not only prevented the formation of β-sheet-rich oligomers, but also destabilized prefibrillar β-sheets via hydrophobic and π–π stacking interactions. Following the above-mentioned two simulation studies, Xie *et al*. examined the influence of the hydroxylated CNT (CNT-OH) on Aβ16–22 aggregation using REMD simulations.[105] Similar to the pristine CNTs, the hydroxylated ones could also inhibit the formation of ordered β-sheet-rich structures. Besides the hydrophobic and aromatic stacking interactions, strong electrostatic interactions between the hydroxyl groups of CNTs and the positively charged residue K16 of Aβ16–22 also played an important role in β-sheet inhibition. Atomic force microscopy and thioflavin T fluorescence experiments by the same authors provide direct evidence of the inhibitory effect of both pristine and hydroxylated CNTs on Aβ16–22 fibrillization.

The absorption of helical Aβ1–42 monomer on CNT surface was studied by Jana *et al*. using MD simulations and the simulations showed that helical Aβ1–42 could be rapidly absorbed on the surface of the nanotube. The CHC region of Aβ was identified as the most favorable interaction site.[106] In addition, the importance of F19 in the interaction of Aβ1–42 with CNT were also examined by the same group with MD simulations of Aβ1–42 mutants.[107]

With the advent of MD simulation studies on Aβ–CNT system, the influence of fullerenes on the structural stability of Aβ protofibrils was also explored by MD simulations. In 2012, Andujar *et al*. studied the interaction between fullerene and Aβ fibrillar structure by the docking method and MD simulations.[108] They found that the binding of C60 to the CHC site caused significant structural alterations of the Aβ protofibrils. Using similar methods, Huy *et al*. studied the binding affinity of Aβ fibril with different sizes of fullerenes ranging from C20 to C84.[109] Compared to other fullerenes, the fullerene C60 is more energetically favorable. In addition, fullerenes have higher binding affinity with Aβ9–40 than with Aβ17–42.

The disruption effect of a soluble fullerene derivative on the Aβ1–42 fibril was investigated by Zhou *et al*. using MD simulations.[110] Three dominant binding sites were identified: the CHC site (^{17}LVFFA^{21}), the turn site (^{27}NKGAI^{31}), and the C-terminal β-sheet site (^{31}IIGLMVGGVVI^{41}). The CHC site is consistent with the one reported previously in the docking study by Andujar *et al.*[108] The other two binding sites, the turn site, and the C-terminal β-sheet site, are newly identified binding sites.[110] Both the aromatic stacking interaction in the CHC site and the curvature matching between fullerene and Aβ1–42 protofibrils played a crucial role for fullerene binding. The binding of fullerene to the turn region disrupted the D23–K28 salt-bridge that is important for the Aβ fibrillation. These simulation results provide an atomic-level explanation for experimentally-observed inhibitory effect of fullerene on Aβ fibrillation.[98]

Conventional MD simulations can be easily trapped in the local free-energy-minimum state. To enhance the conformational sampling, Xie *et al.*, by using REMD simulations, studied the effect of C60 on Aβ16–22 octamerization.[111] Their simulations demonstrated that fullerenes could significantly weaken the inter-peptide interaction and reduce β-sheet propensity, thus leading to disordered oligomers. Interestingly, they found that one C180 molecule displayed stronger inhibitory effect on the β-sheet formation than three C60 molecules (3C60 for short) although they contain the same number of carbon atoms. Fullerene–peptide interaction analyses revealed that the stronger inhibitory effect of C180 on β-sheet formation results from strong hydrophobic and aromatic-stacking interactions between fullerene hexagonal rings and the Phe rings (C180 contains many more hexagonal rings than 3C60).

The influence of carbon nanoparticles (including CNT, CNT-OH, C60, 3C60, and C180) on Aβ16–22 oligomerization is summarized in Fig. 5. It is noted that C180 has approximately the same number of carbon atoms as CNT. Figures 5(a)–5(c) show that CNT, CNT-OH, 3C60, and C180 carbon nanoparticles can significantly reduce the β-sheet content of Aβ16–22. Due to the low C60: peptide molar ratio (1:8), the effect of one C60 molecule on Aβ16–22 octamerization is insignificant. Representative conformations of Aβ16–22 octamers in Fig. 5(d) demonstrate that carbon nanoparticles can shift Aβ16–22 from β-sheet-rich octamers to disordered coil aggregates. Among the four different carbon nanoparticles (CNT, CNT-OH, 3C60, and C180) that contain the same number of carbon atoms, pristine CNT displays the strongest inhibitory effect on the β-sheet formation, followed by C180. The three carbon nanoparticles, CNT, C180, and 3C60, have different surface curvature and consist of different numbers of hexagonal rings. The inhibitory effect relies on the delicate balance of hydrophobic interaction, aromatic stacking, and electrostatic interaction. These results would explain why the four different carbon-nanoparticles display similar interaction mechanism with Aβ but have different inhibitory effect. Other factors, such as surface modification and size effect, would also play roles. Understanding the interaction of carbon nanoparticles with Aβ peptides would provide new information for the development of drugs against Alzheimer's disease.

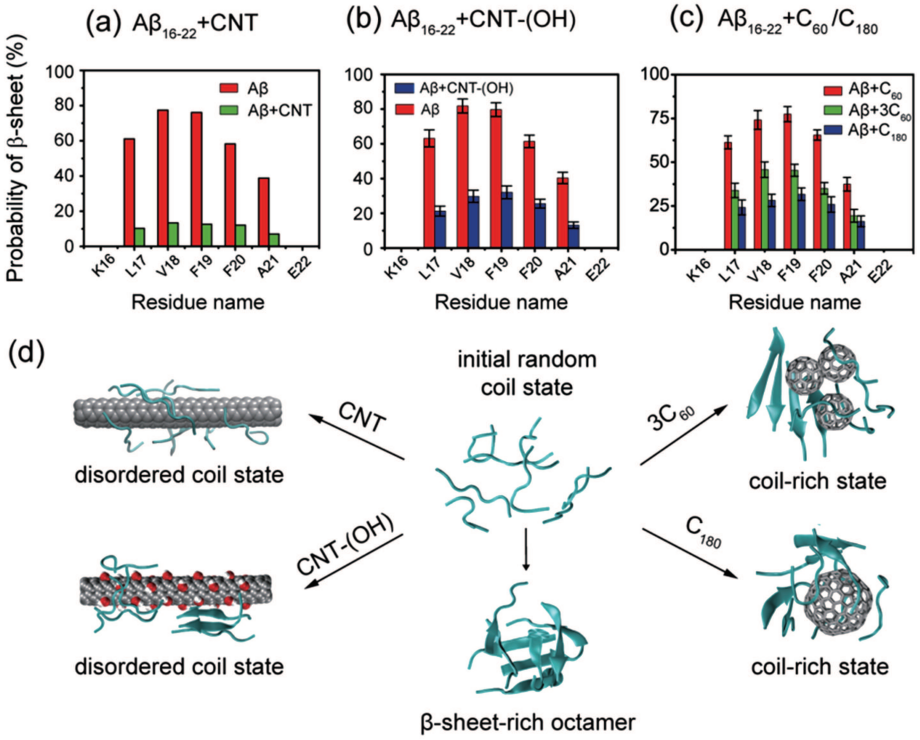


Fig. 5. Effects of different carbon nanoparticles on the oligomerization of Aβ16–22 peptide. The β-sheet propensity of Aβ16–22 octamers is reduced by (a) pristine CNT, (b) CNT-(OH), and (c) three C60 and one C180. Pristine CNTs display the strongest inhibitory effect. (d) Representative conformations of Aβ16–22 octamers in the absence and presence of four different carbon nanoparticles.

5. Conclusions and perspectives

Atomistic MD simulation studies of Aβ aggregation have achieved a great success in various aspects from oligomeric structures to aggregation mechanism in recent years. The REMD method is one of the most suitable strategies to study aggregation of unstructured amyloidogenic peptides. Conformational sampling by REMD was proved to be efficient for short Aβ fragments. Simulation results demonstrate quantitative comparability with experimental results. However, REMD simulations can only provide structural and thermodynamic properties of small oligomers. The kinetics of peptide aggregation is mostly unknown at the atomic level. It is still a challenge for atomistic simulations to uncover the oligomerization process of full-length Aβ. From 2006 to 2015, the simulated system was extended from oligomers of peptide fragment ($<$ 20 aa) to dimers of longer Aβ fragments and full-length Aβ. In the next decade, computational capabilities might enable us to carry out REMD simulations on the oligomerization of multiple full-length Aβ or other peptides. On the one hand, developments in computing ability would provide much information on the early stage of peptide aggregation. On the other hand, more structural information relies on the advances in experimental methods for structural characterization of oligomers. With the rapid development of computing power, improvement of sampling methods, protein force fields, and experimental methods, the processes of Aβ oligomerization, fibril elongation,[112–115] cross-seeding,[116,117] and amyloid inhibition will be uncovered in the near future.

Acknowledgment

Simulations were performed at the National High Performance Computing Center of Fudan University, China.

References

[1] Maji S K, Perrin M H, Sawaya M R, Jessberger S, Vadodaria K, Rissman R A, Singru P S, Nilsson K P, Simon R, Schubert D, Eisenberg D, Rivier J, Sawchenko P, Vale W and Riek R 2009 *Science* **325** 328
[2] Knowles T P, Vendruscolo M and Dobson C M 2014 *Nat. Rev. Mol. Cell Biol.* **15** 384
[3] Selkoe D J 2001 *Physiol. Rev.* **81** 741
[4] Shulman J M, De Jager P L and Feany M B 2011 *Annu. Rev. Pathol.* **6** 193
[5] Prusiner S B 1991 *Science* **252** 1515
[6] Walker F O 2007 *Lancet* **369** 218
[7] Hoppener J W, Ahren B and Lips C J 2000 *N. Engl. J. Med.* **343** 411
[8] Dunker A K, Silman I, Uversky V N and Sussman J L 2008 *Curr. Opin. Struct. Biol.* **18** 756
[9] Sisodia S S, Koo E H, Beyreuther K, Unterbeck A and Price D L 1990 *Science* **248** 492
[10] Buee L, Bussiere T, Buee-Scherrer V, Delacourte A and Hof P R 2000 *Brain Res. Brain Res. Rev.* **33** 95
[11] Westermark P, Wernstedt C, Wilander E, Hayden D W, O'Brien T D and Johnson K H 1987 *Proc. Natl. Acad. Sci. USA* **84** 3881
[12] Spillantini M G, Crowther R A, Jakes R, Hasegawa M and Goedert M 1998 *Proc. Natl. Acad. Sci. USA* **95** 6469
[13] Sunde M, Serpell L C, Bartlam M, Fraser P E, Pepys M B and Blake C C 1997 *J. Mol. Biol.* **273** 729
[14] Jan A, Adolfsson O, Allaman I, Buccarello A L, Magistretti P J, Pfeifer A, Muhs A and Lashuel H A 2011 *J. Biol. Chem.* **286** 8585

[15] Cleary J P, Walsh D M, Hofmeister J J, Shankar G M, Kuskowski M A, Selkoe D J and Ashe K H 2005 *Nat. Neurosci.* **8** 79
[16] Nelson R, Sawaya M R, Balbirnie M, Madsen A O, Riekel C, Grothe R and Eisenberg D 2005 *Nature* **435** 773
[17] Eisenberg D and Jucker M 2012 *Cell* **148** 1188
[18] Sawaya M R, Sambashivan S, Nelson R, Ivanova M I, Sievers S A, Apostol M I, Thompson M J, Balbirnie M, Wiltzius J J, McFarlane H T, Madsen A O, Riekel C and Eisenberg D 2007 *Cah. Rev. The.* **447** 453
[19] Tycko R 2011 *Annu. Rev. Phys. Chem.* **62** 279
[20] Jarrett J T and Lansbury Jr P T 1993 *Cell* **73** 1055
[21] Lomakin A, Teplow D B, Kirschner D A and Benedek G B 1997 *Proc. Natl. Acad. Sci. USA* **94** 7942
[22] Bartolini M, Naldi M, Fiori J, Valle F, Biscarini F, Nicolau D V and Andrisano V 2011 *Anal. Biochem.* **414** 215
[23] DeToma A S, Salamekh S, Ramamoorthy A and Lim M H 2012 *Chem. Soc. Rev.* **41** 608
[24] Theillet F X, Binolfi A, Frembgen-Kesner T, Hingorani K, Sarkar M, Kyne C, Li C, Crowley P B, Gierasch L, Pielak G J, Elcock A H, Gershenson A and Selenko P 2014 *Chem. Rev.* **114** 6661
[25] Curtain C C, Ali F E, Smith D G, Bush A I, Masters C L and Barnham K J 2003 *J. Biol. Chem.* **278** 2977
[26] Aisenbrey C, Borowik T, Bystrom R, Bokvist M, Lindstrom F, Misiak H, Sani M A and Grobner G 2008 *Eur. Biophys. J.* **37** 247
[27] Linse S, Cabaleiro-Lago C, Xue W F, Lynch I, Lindman S, Thulin E, Radford S E and Dawson K A 2007 *Proc. Natl. Acad. Sci. USA* **104** 8691
[28] Cabaleiro-Lago C, Quinlan-Pluck F, Lynch I, Lindman S, Minogue A M, Thulin E, Walsh D M, Dawson K A and Linse S 2008 *J. Am. Chem. Soc.* **130** 15437
[29] Iwatsubo T, Odaka A, Suzuki N, Mizusawa H, Nukina N and Ihara Y 1994 *Neuron* **13** 45
[30] Petkova A T, Ishii Y, Balbach J J, Antzutkin O N, Leapman R D, Delaglio F and Tycko R 2002 *Proc. Natl. Acad. Sci. USA* **99** 16742
[31] Luhrs T, Ritter C, Adrian M, Riek-Loher D, Bohrmann B, Dobeli H, Schubert D and Riek R 2005 *Proc. Natl. Acad. Sci. USA* **102** 17342
[32] Petkova A T, Yau W M and Tycko R 2006 *Biochemistry-us.* **45** 498
[33] Luca S, Yau W M, Leapman R and Tycko R 2007 *Biochemistry-us.* **46** 13505
[34] Andronesi O C, von Bergen M, Biernat J, Seidel K, Griesinger C, Mandelkow E and Baldus M 2008 *J. Am. Chem. Soc.* **130** 5922
[35] Vilar M, Chou H T, Luhrs T, Maji S K, Riek-Loher D, Verel R, Manning G, Stahlberg H and Riek R 2008 *Proc. Natl. Acad. Sci. USA* **105** 8637
[36] Qiang W, Yau W M, Luo Y, Mattson M P and Tycko R 2012 *Proc. Natl. Acad. Sci. USA* **109** 4443
[37] Paravastu A K, Leapman R D, Yau W M and Tycko R 2008 *Proc. Natl. Acad. Sci. USA* **105** 18349
[38] Lu J X, Qiang W, Yau W M, Schwieters C D, Meredith S C and Tycko R 2013 *Cell* **154** 1257
[39] Lindorff-Larsen K, Piana S, Dror R O and Shaw D E 2011 *Science* **334** 517
[40] Morriss-Andrews A and Shea J E 2015 *Annu. Rev. Phys. Chem.* **66** 643
[41] Sugita Y and Okamoto Y 1999 *Chem. Phys. Lett.* **314** 141
[42] Baumketner A, Bernstein S L, Wyttenbach T, Lazo N D, Teplow D B, Bowers M T and Shea J E 2006 *Protein Sci.* **15** 1239
[43] Nishino M, Sugita Y, Yoda T and Okamoto Y 2005 *Febs. Lett.* **579** 5425
[44] Tsai H H, Reches M, Tsai C J, Gunasekaran K, Gazit E and Nussinov R 2005 *Proc. Natl. Acad. Sci. USA* **102** 8174
[45] Sterpone F, Melchionna S, Tuffery P, Pasquali S, Mousseau N, Cragnolini T, Chebaro Y, St-Pierre J F, Kalimeri M, Barducci A, Laurin Y, Tek A, Baaden M, Nguyen P H and Derreumaux P 2014 *Chem. Soc. Rev.* **43** 4871
[46] Cheon M, Chang I and Hall C K 2010 *Proteins* **78** 2950
[47] Wu C and Shea J E 2011 *Curr. Opin. Struct. Biol.* **21** 209
[48] Urbanc B, Cruz L, Teplow D B and Stanley H E 2006 *Curr. Alzheimer Res.* **3** 493
[49] Ma B and Nussinov R 2006 *Curr. Opin. Chem. Biol.* **10** 445
[50] Balbach J J, Ishii Y, Antzutkin O N, Leapman R D, Rizzo N W, Dyda F, Reed J and Tycko R 2000 *Biochemistry* **39** 13748
[51] Ma B and Nussinov R 2002 *Proc. Natl. Acad. Sci. USA* **99** 14126
[52] Ma B and Nussinov R 2006 *Biophys. J.* **90** 3365
[53] Takeda T and Klimov D K 2007 *J. Mol. Biol.* **368** 1202
[54] Gnanakaran S, Nussinov R and Garcia A E 2006 *J. Am. Chem. Soc.* **128** 2158
[55] Wei G and Shea J E 2006 *Biophys. J.* **91** 1638
[56] Wu C, Murray M M, Bernstein S L, Condron M M, Bitan G, Shea J E and Bowers M T 2009 *J. Mol. Biol.* **387** 492
[57] Krone M G, Baumketner A, Bernstein S L, Wyttenbach T, Lazo N D, Teplow D B, Bowers M T and Shea J E 2008 *J. Mol. Biol.* **381** 221
[58] Tarus B, Straub J E and Thirumalai D 2008 *J. Mol. Biol.* **379** 815
[59] Han W and Wu Y D 2005 *J. Am. Chem. Soc.* **127** 15408
[60] Jang S and Shin S 2008 *J. Phys. Chem. B* **112** 3479
[61] Campanera J M and Pouplana R 2010 *Molecules* **15** 2730
[62] Baumketner A and Shea J E 2006 *J. Mol. Biol.* **362** 567
[63] Ikebe J, Kamiya N, Ito J, Shindo H and Higo J 2007 *Protein Sci.* **16** 1596
[64] Baumketner A, Krone M G and Shea J E 2008 *Proc. Natl. Acad. Sci. USA* **105** 6027
[65] Baumketner A and Shea J E 2007 *J. Mol. Biol.* **366** 275
[66] Kittner M and Knecht V 2010 *J. Phys. Chem. B* **114** 15288
[67] Wei G, Jewett A I and Shea J E 2010 *Phys. Chem. Chem. Phys.* **12** 3622
[68] Smith M D, Srinivasa Rao J and Cruz L 2014 *Phys. Chem. Chem. Phys.* **16** 13069
[69] Jang S and Shin S 2006 *J. Phys. Chem. B* **110** 1955
[70] Li H, Luo Y, Derreumaux P and Wei G 2011 *Biophys. J.* **101** 2267
[71] Laganowsky A, Liu C, Sawaya M R, Whitelegge J P, Park J, Zhao M, Pensalfini A, Soriaga A B, Landau M, Teng P K, Cascio D, Glabe C and Eisenberg D 2012 *Science* **335** 1228
[72] Xie L, Luo Y and Wei G 2013 *J. Phys. Chem. B* **117** 10149
[73] Larini L and Shea J E 2012 *Biophys. J.* **103** 576
[74] Cao Z, Liu L, Zhao L and Wang J 2011 *Int. J. Mol. Sci.* **12** 8259
[75] Nguyen P H, Li M S and Derreumaux P 2011 *Phys. Chem. Chem. Phys.* **13** 9778
[76] Baumketner A, Bernstein S L, Wyttenbach T, Bitan G, Teplow D B, Bowers M T and Shea J E 2006 *Protein Sci.* **15** 420
[77] Sgourakis N G, Yan Y, McCallum S A, Wang C and Garcia A E 2007 *J. Mol. Biol.* **368** 1448
[78] Anand P, Nandel F S and Hansmann U H 2008 *J. Chem. Phys.* **128** 165102
[79] Yang M and Teplow D B 2008 *J. Mol. Biol.* **384** 450
[80] Sgourakis N G, Merced-Serrano M, Boutsidis C, Drineas P, Du Z, Wang C and Garcia A E 2011 *J. Mol. Biol.* **405** 570
[81] Roychaudhuri R, Yang M, Deshpande A, Cole G M, Frautschy S, Lomakin A, Benedek G B and Teplow D B 2013 *J. Mol. Biol.* **425** 292
[82] Rosenman D J, Connors C R, Chen W, Wang C and Garcia A E 2013 *J. Mol. Biol.* **425** 3338
[83] Yano A, Okamoto A, Nomura K, Higai S I and Kurita N 2014 *Chem. Phys. Lett.* **595–596** 242
[84] Triguero L, Singh R and Prabhakar R 2008 *J. Phys. Chem. B* **112** 7123
[85] Velez-Vega C and Escobedo F A 2011 *J. Phys. Chem. B* **115** 4900
[86] Lin Y S and Pande V S 2012 *Biophys. J.* **103** L47
[87] Truong P M, Viet M H, Nguyen P H, Hu C K and Li M S 2014 *J. Phys. Chem. B* **118** 8972
[88] Das P, Murray B and Belfort G 2015 *Biophys. J.* **108** 738
[89] Kim S, Takeda T and Klimov D K 2010 *Biophys. J.* **99** 1949
[90] Zhu X, Bora R P, Barman A, Singh R and Prabhakar R 2012 *J. Phys. Chem. B* **116** 4405
[91] Zhang T, Zhang J, Derreumaux P and Mu Y 2013 *J. Phys. Chem. B* **117** 3993
[92] Tarus B, Tran T T, Nasica-Labouze J, Sterpone F, Nguyen P H and Derreumaux P 2015 *J. Phys. Chem. B* **119** 10478
[93] Ball K A, Phillips A H, Nerenberg P S, Fawzi N L, Wemmer D E and Head-Gordon T 2011 *Biochemistry-us.* **50** 7612
[94] Li W, Zhang J, Su Y, Wang J, Qin M and Wang W 2007 *J. Phys. Chem. B* **111** 13814
[95] Nasica-Labouze J, Nguyen P H, Sterpone F, *et al.* 2015 *Chem. Rev.* **115** 3518
[96] Brambilla D, Le Droumaguet B, Nicolas J, Hashemi S H, Wu L P, Moghimi S M, Couvreur P and Andrieux K 2011 *Nanomedicine-Uk* **7** 521
[97] Zaman M, Ahmad E, Qadeer A, Rabbani G and Khan R H 2014 *Int. J. Nanomed.* **9** 899

[98] Kim J E and Lee M 2003 *Biochem. Biophys. Res. Commun.* **303** 576
[99] Podolski I Y, Podlubnaya Z A, Kosenko E A, Mugantseva E A, Makarova E G, Marsagishvili L G, Shpagina M D, Kaminsky Y G, Andrievsky G V and Klochkov V K 2007 *J. Nanosci. Nanotechnol.* **7** 1479
[100] Makarova E G, Gordon R Y and Podolski I Y 2012 *J. Nanosci. Nanotechnol.* **12** 119
[101] Kowalewski T and Holtzman D M 1999 *Proc. Natl. Acad. Sci. USA* **96** 3688
[102] Losic D, Martin L L, Aguilar M I and Small D H 2006 *Biopolymers* **84** 519
[103] Arce F T, Jang H, Ramachandran S, Landon P B, Nussinov R and Lal R 2011 *Soft Matter* **7** 5267
[104] Fu Z, Luo Y, Derreumaux P and Wei G 2009 *Biophys. J.* **97** 1795
[105] Xie L, Lin D, Luo Y, Li H, Yang X and Wei G 2014 *Biophys. J.* **107** 1930
[106] Jana A K and Sengupta N 2012 *Biophys. J.* **102** 1889
[107] Jana A K, Jose J C and Sengupta N 2013 *Phys. Chem. Chem. Phys.* **15** 837
[108] Andujar S A, Lugli F, Hofinger S, Enriz R D and Zerbetto F 2012 *Phys. Chem. Chem. Phys.* **14** 8599
[109] Huy P D and Li M S 2014 *Phys. Chem. Chem. Phys.* **16** 20030
[110] Zhou X, Xi W, Luo Y, Cao S and Wei G 2014 *J. Phys. Chem. B* **118** 6733
[111] Xie L, Luo Y, Lin D, Xi W, Yang X and Wei G 2014 *Nanoscale* **6** 9752
[112] Takeda T and Klimov D K 2009 *Biophys. J.* **96** 442
[113] Han M and Hansmann U H E 2011 *J. Chem. Phys.* **135**
[114] Gurry T and Stultz C M 2014 *Biochemistry-us.* **53** 6981
[115] Han W and Schulten K 2014 *J. Am. Chem. Soc.* **136** 12450
[116] Morales R, Moreno-Gonzalez I and Soto C 2013 *PLoS Pathog.* **9** e1003537
[117] Xi W, Li W and Wang W 2012 *J. Phys. Chem. B* **116** 7398